Bioorganic & Medicinal Chemistry Letters 20 (2010) 4515–4520

Contents lists available at ScienceDirect

Bioorganic & Medicinal Chemistry Letters

journal homepage: www.elsevier.com/locate/bmcl

# NF-κB inducing kinase (NIK) inhibitors: Identification of new scaffolds using virtual screening

Jérémie Mortier [a], Bernard Masereel [a], Caroline Remouchamps [b], Corinne Ganeff [b], Jacques Piette [b], Raphaël frederick [a,*]

[a] Drug Design and Discovery Center, University of Namur, FUNDP, 61 rue de Bruxelles, 5000 Namur, Belgium
[b] Laboratory of Virology and Immunology, GIGA Research, University of Liège, Av de l'Hôpital 1, Bât B34, 4000 Liège, Belgium

ARTICLE INFO

*Article history:*
Received 10 May 2010
Revised 3 June 2010
Accepted 4 June 2010
Available online 8 June 2010

*Keywords:*
NF-κB inducing kinase
NIK
Virtual screening

ABSTRACT

As a wide variety of pro-inflammatory cytokines are involved in the development of rheumatoid arthritis (RA), there is an urgent need for the discovery of novel therapeutic strategies. Among these, the inhibition of the NF-κB inducing kinase (NIK), a key enzyme of the NF-κB alternative pathway activation, represents a potential interesting approach. In fact, NIK is involved downstream of many tumor necrosis factor receptors (TNFR) like CD40, RANK or LTβR, implicated in the pathogenesis of RA. But, up to now, the number of reported putative NIK inhibitors is extremely limited. In this work, we report a virtual screening (VS) study combining various filters including high-throughput docking using a 3D-homology model and ranking by using different scoring functions. This work led to the identification of two molecular fragments, 4*H*-isoquinoline-1,3-dione (**5**) and 2,7-naphthydrine-1,3,6,8-tetrone (**6**) which inhibit NIK with an $IC_{50}$ value of 51 and 90 μM, respectively. This study opens new perspectives in the field of the NF-κB alternative pathway inhibition.



Nuclear factor-κB (NF-κB) has appeared for two decades as one of the most studied mammalian transcription factor. It emerged that NF-κB controls several critical biological functions such as innate and adaptative immunity, cell survival or inflammation.[1,2] Nowadays, it is known that two main pathways control the activation of NF-κB. A wide range of stimuli such as pro-inflammatory cytokines (TNFα, IL-1β, IL-6, CD40L), DNA damaging agents (camptothecin, daunomycin), toll-like receptor (TLR) agonists and viruses trigger the classical NF-κB pathway through pathogen-recognition receptors like TLRs and NACHT-LRRs (NLRs).[3] This pathway (Fig. 1) involves the activation of the IKK complex which phosphorylates IκB members (IκBa, IκBb, IκBe and p105),[4] leading to the ubiquitination and complete degradation of IκBs by the proteasome. Then, free NF-κB complexes enter into the nucleus and gene transcription is initiated.

The alternative NF-κB activation pathway is induced by a subset of tumor necrosis factor ligand (TNFL) family members as well as by some viral proteins.[5] This pathway is dependent on the stabilization and activation of the NF-κB inducing kinase (NIK, Fig. 1). The half-life of this kinase is negatively controlled by TRAF-2, TRAF-3, c-IAP-1 and c-IAP-2.[6,7] Upon activation of receptors like CD40, BAFF or LTβR, the inhibitory function of TRAF-2 and TRAF-3 is alleviated. Then, stabilized NIK activates IKKα leading to the processing of p100 into p52.[8–10] The latter, in association with its main partner Rel-B, fulfils non-redundant biological functions such as secondary lymphoid organ development and induction of specific chemokines involved in adaptive immunity.[5]

Because a wide variety of pro-inflammatory cytokines play a role in the development of rheumatoid arthritis (RA), it might be valuable to design a novel class of inhibitors targeting proteins at the crossroad of multiple pathways relevant to this pathology. Among the potential proteins, NIK certainly represents an attractive candidate since it is involved downstream of many TNFR like CD40, RANK or LTβR implicated in the pathogenesis of RA.

According to our knowledge, only a few series of compounds are claimed as NIK inhibitors. The first that were reported are characterized by a substituted pyrazolo[4,3-*c*]isoquinoline **1** (Fig. 2).[11] However, we recently demonstrated that these compounds were neither inhibitors of NIK nor of the NF-κB alternative activation pathway. In fact, they are inhibitors of another enzyme belonging to the classical NF-κB activation pathway, the TGF-β activated kinase 1 (TAK1).[12] The second series of NIK inhibitors is based on the alkynyl-alcohol moiety **2** (Fig. 2).[13] Unfortunately, neither biological data nor structure–activity relationships related to this series are described in the original patent. Finally, staurosporine **3**, a well-known pan-kinase inhibitor, was also recently shown to be active on NIK.[12]

No X-ray or NMR-structural information of NIK is available. In this context, we recently reported the building of a 3D-model of this kinase using usual homology modeling techniques.[12] This model proved to be relevant to study the binding of potential

* Corresponding author. Tel.: +32 81724290; fax: +32 4 81724299.
*E-mail address:* raphael.frederick@fundp.ac.be (R. frederick).

0960-894X/$ - see front matter © 2010 Elsevier Ltd. All rights reserved.
doi:10.1016/j.bmcl.2010.06.027

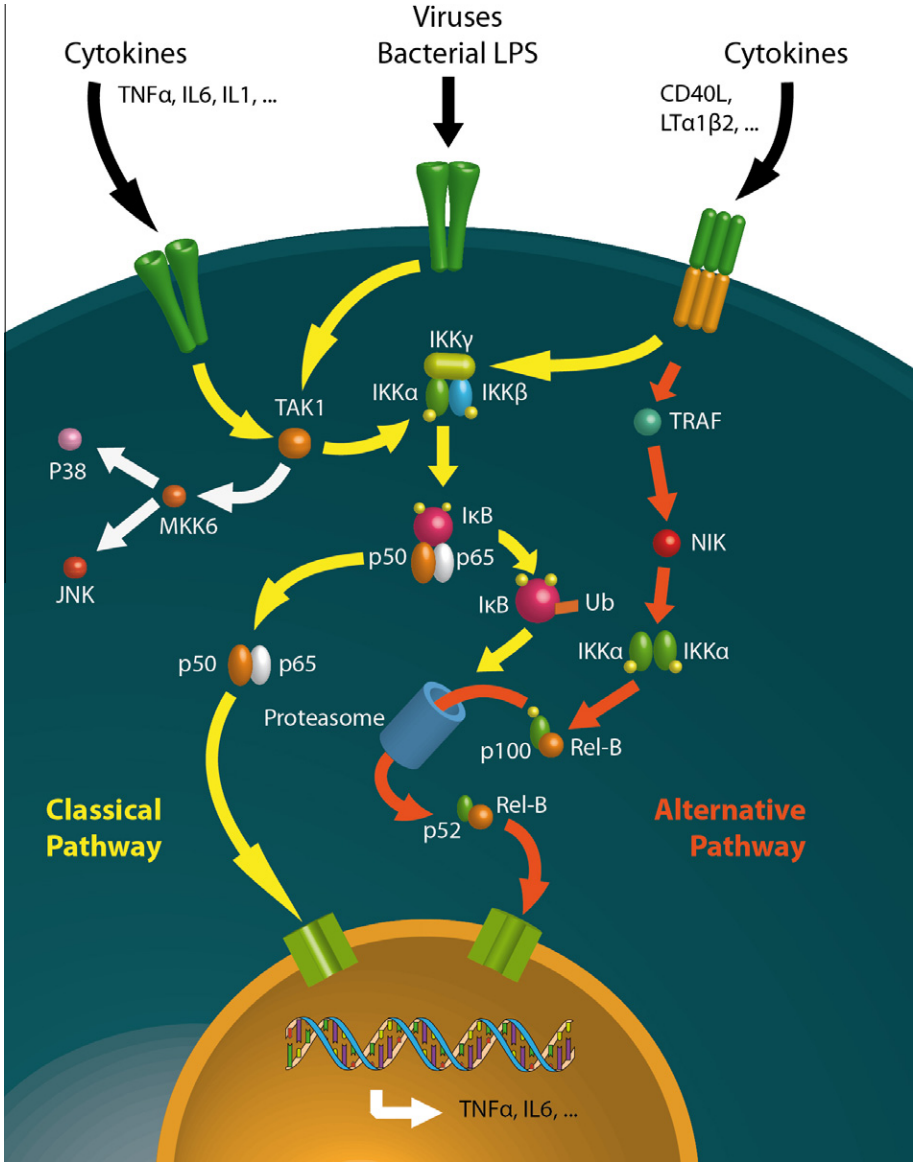


**Figure 1.** Classical (yellow) and alternative (orange) NF-κB activation pathways.

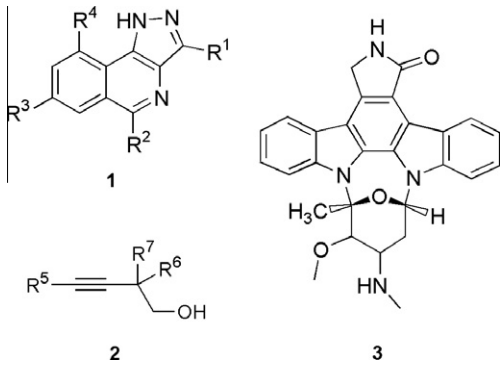


**Figure 2.** NIK inhibitors reported in the literature.

NIK inhibitors. Particularly, it was used to understand, at the molecular level, the essential features required for the stabilization of staurosporine inside the NIK ATP-binding site.[12]

The very limited number of potent NIK inhibitors and an apparently promiscuous enzyme suggested that a broad screening for new scaffolds inhibiting NIK which could be further optimized was a worthwhile challenge for virtual screening (VS).

VS involves the computational screening of very large libraries of commercially-available chemicals that complement targets of known structure, followed by the experimental testing of those with the best predicted binding energies.[14] In the present work, we applied this strategy for the discovery of novel NIK inhibitors, and we identified two novel scaffolds with an inhibitory potency in the 50–100 μM range. To the best of our knowledge, this is the first example of successful VS against NIK.

Various chemical libraries like the NCI database (National Cancer Institute), the ACD (Available Chemical Directory) or the ZINC library (over 8 million commercially-available compounds)[15] can be used to perform VS. The latter, ZINC, was chosen, as it is free, web-accessible, offering ligands in a ready-to-dock 3D format, and as hits are purchasable to evaluate their biological activity.

To increase the rate of hit discovery which can be presumably readily optimiseable in further development, VS focused on small-size molecules, that is, chemical fragments. Various reasons triggered this choice: (i) chemical space can be more efficiently probed by screening collections of small fragments rather than of

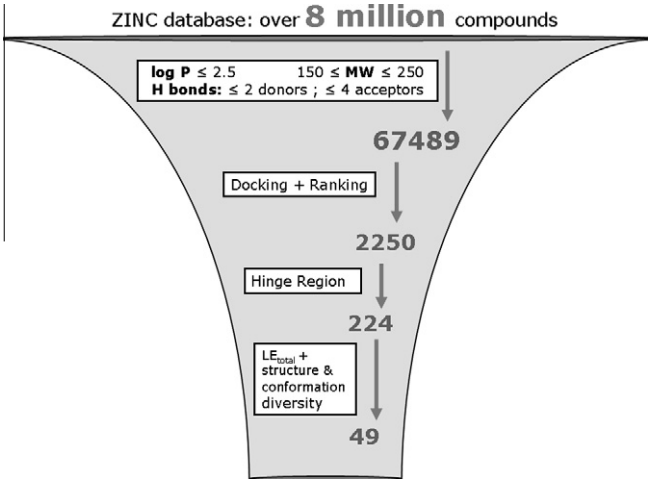


**Figure 3.** Virtual screening flowchart.

libraries of large molecules,[16] (ii) fragments usually present a high ligand efficiency (LE),[17–19] and (iii) this strategy offers an original and unique possibility of designing new leads by fragment evolution or linking.[20] The VS flowchart is depicted in Figure 3.

*First step*: Lipinski-style rules typical for fragments were first applied to the ZINC library.[21,22] The selected descriptors were the molecular weight ($150 < MW < 250$), the hydrophobicity ($\log P \leq 2.5$), and the number of H-bond donors ($HD \leq 2$) and acceptors ($HA \leq 4$). Then, all of the qualified structures were downloaded from the ZINC database and transformed into a *UNITY* hit list file (*SYBYL*)[23] for compatibility with our modeling system. This resulted in a fragment-like library of roughly 67,500 structures (Fig. 3).

*Second step*: The resulting molecules were then docked in the ATP-binding site of NIK using the automated *GOLD* program[24] with parameters especially designed for VS (7–8-fold acceleration). The ATP-binding site of NIK was delimited by a 10 Å-sphere around staurosporine **3**, chosen as reference. For each compound, three docking positions were generated and their affinity with NIK was assessed using three different scoring functions, namely *GOLDSCORE*, *CHEMSCORE* and *ASP*. For each score, a theoretical ligand efficiency index ($LE_{goldscore}$, $LE_{chemscore}$, $LE_{asp}$) was calculated.[19,25,26] Subsequently, a consensus LE index ($LE_{total}$) was obtained by meaning the three individual LE components. Then, the 2000 compounds possessing the best $LE_{total}$, as well as the 100 best compounds in each individual LE, were selected. This led to a set of 2250 structures predicted to tightly bind to NIK.

*Third step*: All these structures were then visually analysed inside the NIK binding cleft, and those that did not interact with the hinge region were discarded. From the resulting 1019 compounds, 324 structures effectively displayed the critical H-bond interaction with the backbone NH of L472, and finally 224 of them were commercially available (Fig. 3).

*Fourth step*: From the last set, 49 compounds were chosen based on structural diversity and appropriate conformation inside the NIK binding cleft. Briefly, the type of interaction of each of the 224 structures in the hinge region was analyzed, and at least one structure per conformation was selected. Additional compounds were also chosen on the basis of their good $LE_{total}$ index. Compounds were bought from different retailers (Chembridge, Enamine, ASDI, IBScreen, Maybridge, Vitas M, Alfa-Aesar, Key Organics, Oakwood, Acros, Sigma–Aldrich, Specs, Asinex and Apollo).

The NIK inhibitory potency of the 49 selected compounds was evaluated using a radiometric protein kinase assay.[27] The residual activity of NIK was measured in presence of the 49 molecules at a single concentration of 50 μM. Briefly, NIK was expressed in Sf9 insect cells as human recombinant GST-fusion protein, and purified

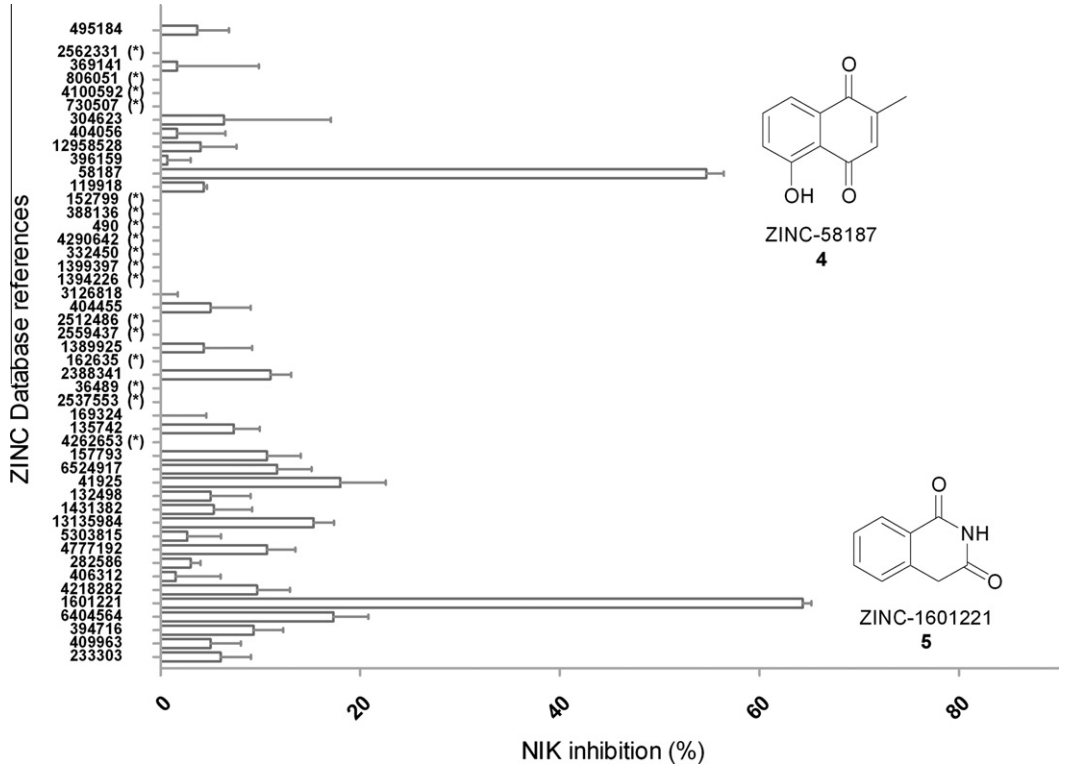


**Figure 4.** Human recombinant NIK inhibition level by the selected 49 compounds (50 μM). Molecules **4** and **5** are the two best inhibitors. (*) denotes a NIK inhibition <0%. Mean ± SD ($n = 3$).

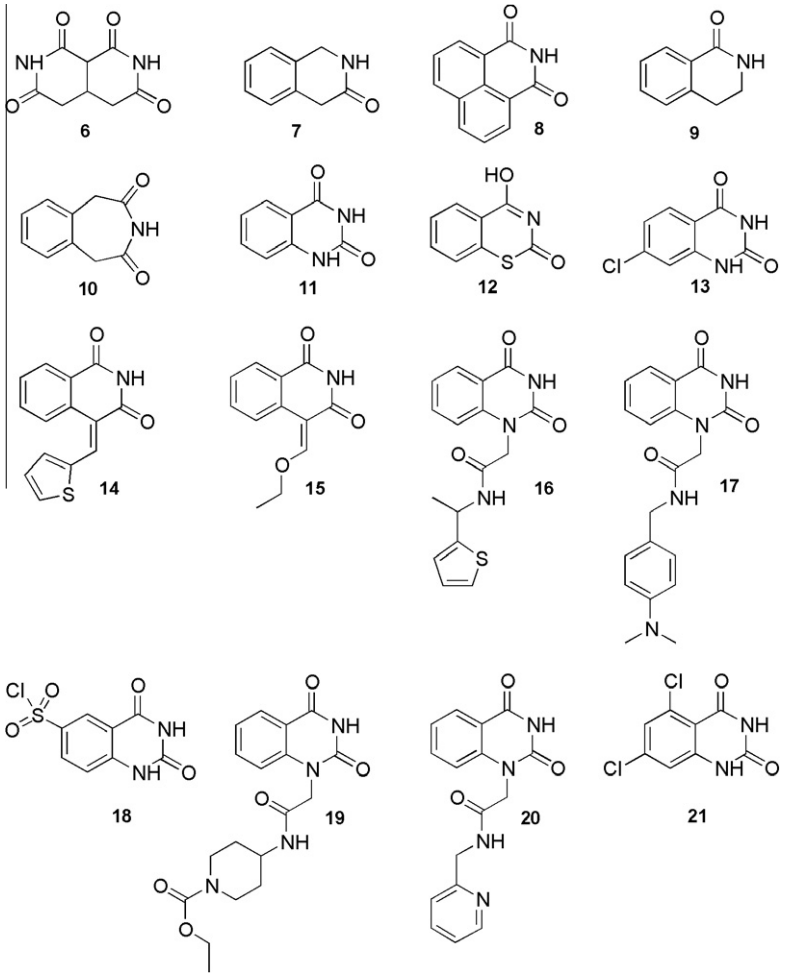


**Figure 5.** Isoquinolinedione related structures **6**–**21**.

by affinity chromatography using GSH-agarose. The substrate, a recombinant protein kinase (RBER-CHKtide) was also expressed in *Escherichia coli*. The assay cocktails were incubated at 30 °C for 60 min with [$\gamma$-$^{33}$P]-ATP (1 μM, pH 7.5) and incorporation of $^{33}$P was measured with a microplate scintillation counter.

From the 49 structures identified by VS, two molecules (**4** and **5**) displayed an interesting NIK inhibitory potency with NIK inhibition of 60% at 50 μM (Fig. 4).

Compound **4** (Fig. 4) is a 1,4-naphthoquinone substituted in the 2- and 5-positions by a methyl and a hydroxyl moiety, respectively. However, quinones are Michael acceptors and well-known as DNA-alkylating agent. They are also highly active as redox molecules and can potentially lead to the formation of reactive oxygen species including superoxide, hydrogen peroxide and hydroxyl radicals. These species in turn can lead to oxidative stress and

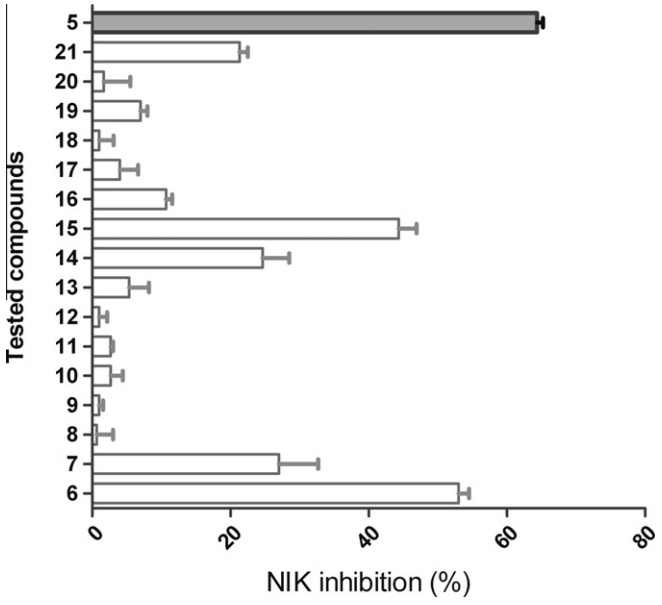


**Figure 6.** NIK inhibitory potency at 50 μM by isoquinolinedione **5** and structurally related compounds. Mean ± SD ($n$ = 3).

**Table 1**
Concentration ($IC_{50}$) reducing of 50% the NIK activity and ligand efficiency index ($LE_{exp}$)

| Compound | $IC_{50}$ (μM) | HA | $LE_{exp} \approx -0.592\ln(IC_{50})/HA$ |
|---|---|---|---|
| Staurosporine | 2.3 | 35 | 0.22 |
| **4** | >100 | 12 | ND |
| **5** | 51 | 14 | 0.42 |
| **6** | 90 | 14 | 0.39 |
| **7** | >100 | 11 | ND |
| **14** | >100 | 18 | ND |
| **15** | >50[a] | 16 | ND |
| **21** | >100 | 14 | ND |

[a] Solubility issues at concentration above 50 μM. HA = number of heavy atoms, $LE_{exp}$ = experimental ligand efficiency, ND = not determined.

the formation of oxidized cellular macromolecules.[28] So, although NIK inhibitor, **4** certainly does not represent an interesting scaffold for future medicinal chemistry development. On the contrary, compound **5**, a 4*H*-isoquinoline-1,3-dione, represents an interesting hit for the discovery of new NIK inhibitors. It should be noted that analogues of this scaffold were recently reported as inhibitors of other kinases such as CDK4 and IGF-1R.[24,29,30]

In order to validate the interest of this new scaffold **5** against NIK, we performed a search for molecules structurally related to this hit. Sixteen commercially-available analogs of **5** were found and purchased (Fig. 5). Their NIK inhibitory potency was then determined (Fig. 6).[27]

At 50 μM, five analogs **6, 7, 14, 15** and **21**, were found to significantly inhibit NIK (>20% inhibition) (Fig. 6). Among them, **6** (53% inhibition @ 50 μM) and **15** (44% inhibition @ 50 μM) seem to be the most potent compounds. Compound **6** possesses a scaffold structurally different from the original 4*H*-isoquinoline-1,3-dione **5**, and therefore could constitute a novel interesting template for the development of novel NIK inhibitors. Compound **15** is an isoquinoline-1,3-dione ring substituted in the 4-position by an ethoxymethylene group. It is interesting to note that the substitution in this position seems tolerated but only with a rather small group. Indeed, except compound **14** (25% inhibition @ 50 μM) substituted by a thiophenylmethylene moiety in this position, molecules **16**, **17**, **19** and **20**, bearing a bulkier group, are completely inactive on NIK (inhibition <15% @ 50 μM). Another hypothesis to explain the activity of **14–15** is the presence of a Michael acceptor exocyclic double bond which is not present in **16**, **17**, **19** and **20** (Figs. 5 and 6). This reactive Michael acceptor might play a role in the binding of these derivatives.

The dose–response inhibitory potency of the most interesting compounds was performed. The required concentration ($IC_{50}$) to reduce of 50% the NIK activity was evaluated for compounds **4–7**, **14**, **15**, **21**, and compared to that of staurosporine chosen as reference (Table 1). Although less potent than staurosporine, **5** remains the most promising NIK inhibitor with an $IC_{50}$ value of 51 μM. The inhibitory potency of 2,7-naphthyridine-1,3,6,8-tetrone **6** is less potent with an $IC_{50}$ of 90 μM. Compounds **4**, **7**, **14**, **15**, and **21** possess $IC_{50}$'s >100 μM. As a parameter for assay quality, the Z′-factor was used for the low and high controls of each assay plate.[31] Our criterion for repetition of an assayed plate is a Z′-factor lower than 0.4.[32] In this experiment, Z′-factors did not drop below 0.77, indicating an excellent assay quality. As an additional control, a 1% DMSO plate was included as an indicator for putative washing and/or pipetting variations. The calculated coefficient of variation was 5.01%.

Interestingly, compounds **5** and **6** are characterized by a high ligand efficiency index ($LE_{exp}$), defined as the ratio between their potency and their number of heavy atoms (HA).[17,18] The $LE_{exp}$ of **5** and **6** is 0.42 and 0.39, respectively, whereas the $LE_{exp}$ of staurosporine is only 0.22 (Table 1). So, the $LE_{exp}$ of **5** and **6** reaches the minimum value of 0.3 usually reported for a hit to be considered as an interesting starting point for further drug development.[20]

To understand how these two compounds achieve their potency, we investigated their binding conformation inside the NIK cavity. Both molecules were docked inside the NIK-binding site according to the methodology described. In order to take into account the protein flexibility, the best conformation was further refined using the *MINIMIZE* module implemented in *SYBYL* 8.0 (Tripos force field and Gasteiger-Hückel charges). Key interactions stabilizing the compounds **5** and **6** are depicted in Figure 7.

Both inhibitors are deeply inserted in the NIK cavity. As expected, for each compound, one H-bond acceptor atom, that is, the oxygen atom from the carbonyl in position 1, onto the ligand is H-bonded to the L472 backbone NH located in the NIK hinge region (ATP-binding site). Additionally, both compounds also appear to be stabilized through a supplementary H-bond between the nitrogen atom in position 2 of the ligand regarded as H-bond donor, and the L472 CO backbone considered as H-bond acceptor. Except these two H-bonds, the NIK inhibitory potency could be attributed mainly to the close shape complementarities and van der Waals contacts between these two inhibitors and the NIK active site (Fig. 7).

In conclusion, a virtual screen (VS) combining various filters including high-throughput docking using a 3D-homology model and ranking through different scoring functions was used to search for new NIK inhibitors. From the 49 final compounds identified and assayed, two molecules exhibited a NIK inhibitory potency of about 50% at 50 μM, one of them (**5**) being characterized by an $IC_{50}$ of 51 μM. This corresponds to an enrichment rate of about 2%. Although enrichment rates in the range of 10–30% were previously reported by VS using experimentally determined 3D structures, this is still an interesting rate especially taking into account the use of a homology model but not experimental 3D-coordinates of NIK for the VS. Also, although care must be taken when comparing hit rates from VS and HTS as **5** has not yet been confirmed for reversibility and ATP-competition and the concentration used for screening in HTS is usually lower that 50 μM (used in the present screening), our strategy afforded one active scaffold after the testing of only 49 derivatives compared to a hit rate of about 0.02% for HTS in most cases.[14] The present study is therefore another example highlighting the excellent capabilities of VS for the discovery of

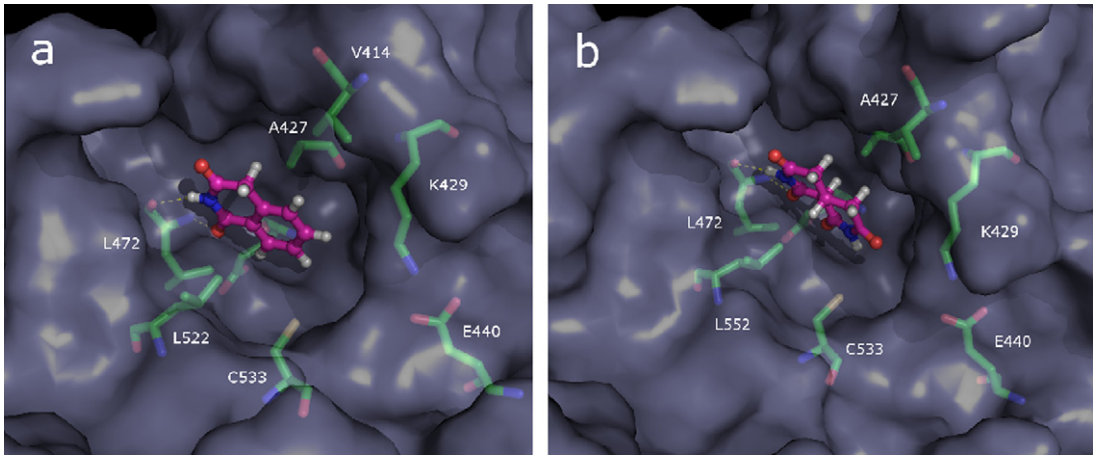


**Figure 7.** NIK inhibitors **5** (a) and **6** (b) docked in the ATP-binding site of NIK.

novel hits. Structural analogues of **5** were then searched and led to the identification **6** endowed with an inhibitory potency around 90 μM. Interestingly, these two chemical fragments (**5** and **6**) are characterized by a good experimental ligand efficiency ($LE_{exp}$) compared to that of staurosporine, the best inhibitor of NIK reported so far. The binding modes of these two molecules within NIK were finally evaluated, and revealed essential features responsible for their NIK inhibition potency. Particularly, these compounds interact with the hinge region of NIK via a lactam moiety, similarly to staurosporine which is known to be an ATP-competitive pan-kinase inhibitor. Based on this observation, it could be hypothesized that these molecules inhibit NIK with a similar mechanism.

This work is still in progress and analogues of **5** are currently being designed based on its binding orientation in the NIK ATP-binding site. Once more potent compounds will be obtained, the mechanism of action in this series will be investigated in more details.

## Acknowledgments

The authors would like to acknowledge Dr. Emmanuel Dejardin for fruitful discussions. This work was funded by the Walloon Region (PRALTER no 0516272). R.F. is greatly indebted to the Belgian 'Fonds de la Recherche Scientifique—FNRS' for the award of a post-doctoral research grant.

## References and notes

1. Ghosh, S.; Karin, M. *Cell* **2002**, *109*, S81.
2. Hayden, M. S.; Ghosh, S. *Gene Dev.* **2004**, *18*, 2195.
3. Martinon, F.; Tschopp, J. *Trends Immunol.* **2005**, *26*, 447.
4. Karin, M.; Ben-Neriah, Y. *Annu. Rev. Immunol.* **2000**, *18*, 621.
5. Dejardin, E. *Biochem. Pharmacol.* **2006**, *72*, 1161.
6. Vallabhapurapu, S.; Matsuzawa, A.; Zhang, W.; Tseng, P. H.; Keats, J. J.; Wang, H.; Vignali, D. A.; Bergsagel, P. L.; Karin, M. *Nat. Immunol.* **2008**, *9*, 1364.
7. Liao, G. X.; Zhang, M. Y.; Harhaj, E. W.; Sun, S. C. *J. Biol. Chem.* **2004**, *279*, 26243.
8. Claudio, E.; Brown, K.; Park, S.; Wang, H.; Siebenlist, U. *Nat. Immunol.* **2002**, *3*, 958.
9. Coope, H. J.; Atkinson, P. G.; Huhse, B.; Belich, M.; Janzen, J.; Holman, M. J.; Klaus, G. G.; Johnston, L. H.; Ley, S. C. *EMBO J.* **2002**, *21*, 5375.
10. Dejardin, E.; Droin, N. M.; Delhase, M.; Haas, E.; Cao, Y.; Makris, C.; Li, Z. W.; Karin, M.; Ware, C. F.; Green, D. R. *Immunity* **2002**, *17*, 525.
11. Flohr, S. N., T. US 6,841,556 B2, 2005.
12. Mortier, J.; Frederick, R.; Ganeff, C.; Remouchamps, C.; Talaga, P.; Pochet, L.; Wouters, J.; Piette, J.; Dejardin, E.; Masereel, B. *Biochem. Pharmacol.* **2010**, *79*, 1462.
13. Chen, G.; Cushing, T. D.; Fisher, B.; He, X.; Li, K.; Li, Z.; McGee, L., R. WO 2009/158011 A1, 2009.
14. Shoichet, B. K. *Nature* **2004**, *432*, 862.
15. Irwin, J. J.; Shoichet, B. K. *J. Chem. Inf. Comput. Sci.* **2005**, *45*, 177.
16. Rees, D. C.; Congreve, M.; Murray, C. W.; Carr, R. *Nat. Rev. Drug Disc.* **2004**, *3*, 660.
17. Abad-Zapatero, C.; Metz, J. T. *Drug Discovery Today* **2005**, *10*, 464.
18. The ligand efficiency (LE) is the binding free energy for a ligand divided by its molecular size. $LE = -\Delta G/HA \approx -RT\ln(IC_{50})/HA \approx -0.592\ln(IC_{50})/HA = LE_{exp}$. LE is a useful metric for measuring the impact on activity of the addition of more molecular bulk. Molecules that achieve a given potency with fewer heavy atoms are by definition more efficient.
19. Reynolds, C. H.; Tounge, B. A.; Bembenek, S. D. *J. Med. Chem.* **2008**, *51*, 2432.
20. Congreve, M.; Chessari, G.; Tisi, D.; Woodhead, A. J. *J. Med. Chem.* **2008**, *51*, 3661.
21. Lipinski, C. A.; Lombardo, F.; Dominy, B. W.; Feeney, P. J. *Adv. Drug Delivery Rev.* **1997**, *23*, 3.
22. Teague, S. J.; Davis, A. M.; Leeson, P. D.; Oprea, T. *Angew. Chem., Int. Ed.* **1999**, *38*, 3743.
23. Tripos, I. SYBYL: 1699 South Hanley Rd., St. Louis, Missouri, 63144, USA.
24. Jones, G.; Willett, P.; Glen, R. C.; Leach, A. R.; Taylor, R. *J. Mol. Biol.* **1997**, *267*, 727.
25. The theoretical ligand efficiency ($LE_{score}$) is obtained by dividing the affinity score value by the MW of the compound ($LE_{score}$ = score/MW).
26. Hopkins, A. L.; Groom, C. R.; Alex, A. *Drug Discovery Today* **2004**, *9*, 430.
27. This assay was performed by ProQinase using $^{33}$PanQinase technology. Inhibitory potency of staurosporine and of the 49 molecules identified from VS was evaluated at 50 μM on human recombinant NIK. DMSO was used as co-solvent and its final concentration was 1%. NIK was expressed in Sf9 insect cells as human recombinant GST-fusion protein. The kinase was purified by affinity chromatography using GSH-agarose. The purity of the kinase was checked by SDS–PAGE/silver staining and the identity was verified by mass spectroscopy. The NIK activity was measured as the incorporation on an artificial substrate of $^{33}$P produced by hydrolysis of [γ-$^{33}$P]-ATP. The substrate (RBER-CHKtide) was an artificial fusion protein expressed in *Escherichia coli*. It was consisting of a *N*-terminal GSTtag separated by a thrombin cleavage site from a fragment of the human retinoblastoma protein RB1, amino acids S773-K928 followed by 11 Arg residues (ER) and a peptide sequence KKKVRSGLYRSPSMPENLNRPR (CHKtide).
28. Bolton, J. L.; Trush, M. A.; Penning, T. M.; Dryhurst, G.; Monks, T. J. *Chem. Res. Toxicol.* **2000**, *13*, 135.
29. Tsou, H. R.; Otteng, M.; Tran, T.; Floyd, M. B.; Reich, M.; Birnberg, G.; Kutterer, K.; Ayral-Kaloustian, S.; Ravi, M.; Nilakantan, R.; Grillo, M.; McGinnis, J. P.; Rabindran, S. K. *J. Med. Chem.* **2008**, *51*, 3507.
30. Tsou, H. R.; Liu, X.; Birnberg, G.; Kaplan, J.; Otteng, M.; Tran, T.; Kutterer, K.; Tang, Z. L.; Suayan, R.; Zask, A.; Ravi, M.; Bretz, A.; Grillo, M.; McGinnis, J. P.; Rabindran, S. K.; Ayral-Kaloustian, S.; Mansour, T. S. *J. Med. Chem.* **2009**, *52*, 2289.
31. Zhang, J. H.; Chung, T. D.; Oldenburg, K. R. *J. Biomol. Screening* **1999**, *4*, 67.
32. Iversen, P. W.; Eastwood, B. J.; Sittampalam, G. S.; Cox, K. L. *J. Biomol. Screening* **2006**, *11*, 247.